HHS Public Access

Author manuscript

Oncogene. Author manuscript; available in PMC 2023 May 01.

Published in final edited form as:

Oncogene. 2022 November ; 41(48): 5214–5222. doi:10.1038/s41388-022-02500-w.

STAT5 confers lactogenic properties in breast tumorigenesis and restricts metastatic potential

Meng Lin[1,2,*], **Amy T. Ku**[1,*], **Jie Dong**[1], **Fei Yue**[1,3], **Weiyu Jiang**[1], **Ahmed Atef Ibrahim**[1], **Fanglue Peng**[4], **Chad J. Creighton**[3,5], **Chandandeep Nagi**[6], **Carolina Gutierrez**[1], **Jeffrey M. Rosen**[3,4], **Xiang H.-F. Zhang**[1,4,5], **Susan G. Hilsenbeck**[1,3,5], **Xi Chen**[4,5], **Yi-Chieh Nancy Du**[7], **Shixia Huang**[3,4,5,8], **Aiping Shi**[2], **Zhimin Fan**[2], **Yi Li**[1,4,5]

[1]Lester and Sue Smith Breast Center, Baylor College of Medicine, Houston, TX, USA

[2]Department of Breast Surgery, General Surgery Center, the First Hospital of Jilin University, Changchun, Jilin, China

[3]Department of Medicine, Baylor College of Medicine, Houston, TX, USA

[4]Department of Molecular and Cellular Biology, Baylor College of Medicine, Houston, TX, USA

[5]Dan L. Duncan Comprehensive Cancer Center, Baylor College of Medicine, Houston, TX, USA

[6]Department of Pathology and Immunology, Baylor College of Medicine, Houston, TX, USA

[7]Department of Pathology and Laboratory Medicine, Weill Cornell Medicine, New York, NY, USA

[8]Department of Education, Innovation & Technology, Houston, TX, USA

Abstract

Signal transducer and activator of transcription 5 (STAT5) promotes cell survival and instigates breast tumor formation, and in the normal breast it also drives alveolar differentiation and lactogenesis. However, whether STAT5 drives a differentiated phenotype in breast tumorigenesis and therefore impacts cancer spread and metastasis is unclear. We found in two genetically engineered mouse models of breast cancer that constitutively activated *Stat5a* (*Stat5a*^{ca}) caused precancerous mammary epithelial cells to become lactogenic and evolve into tumors with diminished potential to metastasize. We also showed that STAT5a^{ca} reduced the migratory and invasive ability of human breast cancer cell lines *in vitro*. Furthermore, we demonstrated that STAT5a^{ca} overexpression in human breast cancer cells lowered their metastatic burden in

Corresponding author: Yi Li, PhD, Baylor College of Medicine, 1 Baylor Plaza, BCM 600, Alkek N1220.06, Houston, TX, 77030, USA, liyi@bcm.edu.

*These authors contributed equally to this manuscript

Contributions

ML, ATK, JD contributed to the experimental design, methodology, data acquisition and analysis. WJ and AAI contributed to data acquisition in animal work. CN and CG evaluated slides and provided pathological reports. FY, FP and CJC performed bio-informatic analyses. SGH supervised statistical analyses. ML, ATK, and YL wrote the manuscript. JMR, XHZ, XC, YND, SH, AS and ZF provided supervision. All authors read the manuscript, agreed with the content, and were given the opportunity to provide input.

Ethics approval and consent to participate

All animal procedures were performed under the institutional animal care and use committee of Baylor College of Medicine with the recommendations in the Guide for care and Use of Laboratory Animals.

Conflicts of interest

Authors declare that they have no conflicts of interest.

xenografted mice. Moreover, RPPA, Western blotting, and studies of ChIPseq data identified several EMT drivers regulated by STAT5. In addition, bioinformatic studies detected a correlation between STAT5 activity and better prognosis of breast cancer patients. Together, we conclude that STAT5 activation during mammary tumorigenesis specifies a tumor phenotype of lactogenic differentiation, suppresses EMT, and diminishes potential for subsequent metastasis.

Keywords

STAT5; Breast cancer; Differentiation; Metastasis; Epithelial-mesenchymal transition

INTRODUCTION

The STAT family of transcriptional factors comprises STAT1, 2, 3, 4, 5A, 5B, and 6 [1]. STAT5a is the principal STAT family member expressed in the mammary glands at all stages of mammary development except during involution [2]. It is usually phosphorylated and activated by Janus kinase 2 (JAK2) following prolactin and other cytokine hormones binding to their cognate receptors. Phosphorylated STAT5a proteins then homodimerize (or sometimes heterodimerize with another family member), translocate to the nucleus, and transactivate genes that regulate lobuloalveolar formation and milk production as well as cell survival, as we and others have reported [3–6].

Although not often mutated, STAT5 (referring to STAT5a/b as most commercial antibodies cannot distinguish these two highly homologous proteins) is known to be activated in breast atypia [7], ductal carcinoma in situ (DCIS) [8], and between 20 and 70% of human breast cancers [9–11]. pSTAT5 is found primarily in estrogen receptor α positive (ERα+) mammary tumors, but also in a subset of HER2+ tumors as well as triple-negative breast cancer (TNBC) [9–11]. The oncogenic potential of this lactogenic protein has been tested in animal models. STAT5a activation alone does not generally transform mammary cells [6, 8] although there are a few reports suggesting that transgenic expression of activated or even wild-type *Stat5a* in mice may lead to mammary tumors in a small proportion of the mice with a long latency [12–14]. On the other hand, constitutively activated *Stat5a* (*Stat5a*^{ca}) can potently accelerate mammary tumorigenesis initiated by an oncogene such as *ErbB2* (*HER2*), likely via transactivation of anti-apoptosis genes that lower the apoptosis anticancer barrier often activated during tumor initiation [8].

While STAT5 can instigate breast tumor formation, STAT5 and nuclear STAT5 were detected less in high-grade breast cancer than in low-grade tumors, less in invasive carcinomas than in the prognostically more favorable secretory carcinoma subtype, and less in metastases than in primary tumors [9–11, 15, 16]. Higher STAT5 or pSTAT5 levels are also correlated with better patient overall and disease-specific survivals [10, 11, 15, 16]. These association studies suggest that STAT5 may be a favorable prognostic factor. In accordance, a few in vitro studies also showed that activation of PRL-JAK2-STAT5 signaling in cultured breast tumor cells can induce alveolar differentiation and suppress migration, invasion, and epithelial to mesenchymal transition (EMT) [17–19], but *in vivo* evidence confirming these observations is lacking. On the contrary, in two experimental

metastasis mouse models, STAT5 was found to stimulate triple-negative breast cancer bone metastasis [20] and prostate cancer lung metastasis [21]. Furthermore, in clinical studies, high STAT5 activity was associated with advanced stage and poor outcome of prostate [22] and hepatocellular carcinoma [23]. Besides, STAT5 has been reported to promote EMT in several cancers of non-breast origin [21, 23–26]. Nonetheless, it remains unclear whether STAT5 activation drives alveolar and lactogenic differentiation during breast tumorigenesis and whether STAT5 affects metastasis of breast cancer *in vivo*.

In this study, we investigated the causal roles of STAT5a (the predominant isoform of STAT5) in alveolar and lactogenic differentiation during mammary tumorigenesis and progression in two different mouse models of breast cancer and in human breast cells cultured *in vitro* and as xenografts. We also studied potential mechanisms and their implications in breast cancer patients. These studies have uncovered a dichotomous function of STAT5 in breast tumorigenesis and metastasis.

RESULTS AND DISCUSSION

STAT5a activation causes alveolar differentiation of precancerous mammary lesions initiated by *ErbB2*

We previously reported that mammary intraductal injection of a Rous Sarcoma virus-derived vector (RCAS) can be used to deliver genes into the mouse mammary epithelia made susceptible to infection by transgenic expression of *tva* (encoding the receptor for RCAS) using the MMTV LTR promoter [27]. RCAS-mediated expression of a gene encoding a constitutively activated version of *Stat5a* (*Stat5a*^{ca}) drove alveolar differentiation and milk production in the absence of a pregnancy but rarely, if ever, induced precancerous lesions or tumors after many months [6, 8]. On the other hand, two weeks after intraductal injection of both RCAS-FLAG-*Stat5a*^{ca} and RCAS-HA-*ErbB2*^{ca}, precancerous lesions (defined as at least 3 layers of atypical cells growing into lumen [8]) were detectable by H&E staining (Fig. S1A) and 31% of these lesions were positive for both HA and FLAG (Fig. S1B, S1C). To test whether STAT5a affects the differentiation status of precancerous cells, we stained these lesions for two differentiation markers associated with milk production, β-casein and perilipin-2 (PLIN2, or adipophilin). We found abundant amounts of β-casein and PLIN2 in lesions positive for both ErbB2^{ca} and STAT5a^{ca}, but much less expression in lesions positive for ErbB2^{ca} only (Fig. 1A, S1D). These data demonstrate that STAT5a activation in precancerous lesions specifies an alveolar and lactogenic fate to the cells, similar to the impact of the STAT5 activation in the normal epithelial cells [6, 28].

STAT5 activation leads to a functionally differentiated tumor phenotype

We previously reported that STAT5a activation accelerated tumorigenesis initiated by *ErbB2*^{ca} based on the observation that MMTV-*tva* female mice co-injected with RCAS-HA-*ErbB2*^{ca} and RCAS-FLAG-*Stat5a*^{ca} developed mammary tumors significantly faster than age-matched MMTV-*tva* mice injected with RCAS-*ErbB2*^{ca} alone [8]. These data predicted that the small proportion of co-infected cells (approximately 8% [8]) were much more competitive in tumorigenesis than cells expressing ErbB2^{ca} only. Immunohistochemistry for HA and FLAG on the tumors from the co-infected mice detected double positivity

in 7 of 13 (53.8%) tumors while the remaining 6 tumors (46.2%) expressed ErbB2^{ca} only (Fig. S1E, S1F). And 5 of the 7 double-positive tumors exhibited near uniform positivity for FLAG, compared to moderate proportion scores in precancerous lesions (Fig. S1G). As expected, Kaplan-Meier tumor-free survival curves of mice bearing ErbB2^{ca}+/STAT5a^{ca}+ tumors separated well from those of mice bearing ErbB2^{ca}+/STAT5a^{ca}- tumors, which became inseparable from that of age-matched mice infected by RCAS-*ErbB2*^{ca} alone (Fig. S2A). In accordance with our previous report of STAT5 primarily promoting tumorigenesis via suppressing the apoptosis anticancer barrier (rather than proliferation) [8], ErbB2^{ca}+/STAT5a^{ca}+ tumors produced increased levels of BCL2 and BCL-xL (BCL2L1) (Fig. S2B, S2C), pro-survival proteins reported to be STAT5 targets [29, 30] although this transcriptional control has been controversial [31]. We next examined whether STAT5 activation also specifies a differentiated mammary tumor phenotype. Immunohistochemistry confirmed robust expression of both β-casein and PLIN2 in all 5 STAT5a^{ca}+ tumors examined while 3 of 5 STAT5a^{ca}- tumors didn't show any β-casein expression, and 4 of 5 exhibited low levels of PLIN2 (Fig. 1A). Together, while confirming our previous observation that STAT5 activation accelerates *ErbB2*-initiated tumorigenesis likely by suppressing the anticancer barrier, these data show that STAT5 induces a functionally differentiated phenotype of tumors initiated by ErbB2 activation.

Activation of STAT5a during tumor initiation restricts the metastatic potential of HER2+ mammary tumors in mice

To test whether STAT5a-caused functional differentiation in tumor cells affects their metastatic potential, we compared the tumor burden in lungs by H&E. Figure 1B shows representative images of H&E staining of lungs at euthanasia when the primary ErbB2^{ca}+ tumors with or without STAT5a^{ca} reached 1.5 cm in diameter. Twelve of 30 (40 %) mice bearing ErbB2^{ca}-only mammary tumors harbored nests of tumor cells in the lungs. In contrast, only 1 of 16 (6.25%) mice bearing ErbB2^{ca}+/STAT5a^{ca}+ tumors presented tumor nests in the lungs (Fig. 1C). This 6-fold decrease of lung metastases suggests that the activation of STAT5 restricts the metastatic potential of *ErbB2*-initiated mammary tumors.

STAT5a overexpression leads to a more functionally differentiated tumor phenotype of ER+ breast cancer initiated by *PIK3CA*^{H1047R}

To test whether this STAT5 impact on tumor cell differentiation and metastasis is broadly applicable among a wide range of breast tumors, we tested the effects of STAT5 activation in mammary tumors initiated by *PIK3CA*, the proto-oncogene mostly commonly mutated in human breast cancer, especially in the ER+ subtype [32]. *PIK3CA* is too large to be expressed using RCAS, but we have reported that intraductal injection of lentivirus (FUCGW) carrying *PIK3CA*^{H1047R}, leads to ER+ mammary tumors in mice [33], while others have reported similar tumors using transgenic expression of mutated *PIK3CA* [34, 35]. Therefore, we intraductally injected FUCGW-*PIK3CA*^{H1047R} alone or together with FUW-FLAG-*Stat5a*^{ca} into the mammary glands of FVB female mice, and compared the features of the resulting mammary tumors by H&E staining and immunostaining. All 8 tumors initiated by *PIK3CA*^{H1047R} alone were well differentiated ductal carcinoma with extensive glandular formation, in accordance with our previous report of tumors induced by FUCGW-*PIK3CA*^{H1047R} [33]. All 8 tumors in mice co-injected with both

viruses produced both PIK3CA^{H1047R} and STAT5a^{ca}, highlighting their collaborative roles in mammary tumorigenesis (Fig. 2). Besides, all STAT5a^{ca}+ tumors exhibited advanced pathological features including high-grade nuclear pleomorphism, high mitotic rates (>15 mitoses per 10 HPF's), extensive areas of necrosis, and some metaplastic areas of squamous differentiation (Fig. 2). (This increase in aggressive pathological features was not observed in comparing tumors initiated by *ErbB2^{ca}* vs. *ErbB2^{ca}*/*Stat5a^{ca}*.) However, these PIK3CA^{H1047R}/STAT5a^{ca} tumors remained ERα+ (Fig. 2). Consistent with our observation in tumors initiated by both *ErbB2^{ca}* and *Stat5a^{ca}*, all 8 PIK3CA^{H1047R}/STAT5a^{ca} tumors exhibited robust expression of both β-casein and PLIN2, indicative of elevated lactogenic differentiation, while all 6 PIK3CA^{H1047R} only tumors showed negligible β-casein and PLIN2 expression (Fig. 2). However, we could not assess the impact of STAT5a^{ca} on metastasis in this model, since mice bearing PIK3CA^{H1047R}-only tumors or PIK3CA^{H1047R}/STAT5a^{ca} tumors did not develop detectable lung metastases at the ethnical end point of primary tumors reaching 2.0 cm in diameter. Together, these data suggest that STAT5 activation causes a more functionally differentiated phenotype in mammary tumors initiated by PIK3CA activation although the tumors with higher STAT5 activity appear more aggressive histopathologically.

Activation of STAT5a restricts the metastatic potential of human breast cancer cells in vitro and in vivo

To determine whether STAT5 activation affects the metastatic ability of human breast tumor cells, we stably introduced STAT5a^{ca} using a lentiviral vector into two human breast lines and compared their migratory and invasive capacity with their corresponding control cells. STAT5a^{ca} decreased the migration and invasion abilities of MCF10A-PIK3CA^{H1047R} by approximately 70-80% (Fig. 3A, 3B, S3A), and those of MCF7 by approximately 50% (Fig. S3B) while STAT5a^{ca} didn't affect the growth of MCF10A cells (Fig. S3C). Furthermore, we compared two MCF10A cell sublines in a 3D Matrigel culture. While both MCF10A-PIK3CA^{H1047R} and MCF10A-PIK3CA^{H1047R}/STAT5a^{ca} grew similarly shaped spheres initially (day 4), with time, the former developed invasive protrusions while the latter remained spherical (Fig S3D). These *in vitro* data suggest that STAT5a hinders breast cancer metastasis.

Next, we tested whether STAT5a^{ca} affects human breast cancer metastasis *in vivo*. We intraductally implanted MCF10A-PIK3CA^{H1047R} cells and MCF10A-PIK3CA^{H1047R}/STAT5a^{ca} cells into the #4 mammary glands of female NSG mice. IVIS imaging and tumor palpation indicate that STAT5a^{ca} does not significantly impact the growth of these MCF10A-PIK3CA^{H1047R} cells (Fig. S4A, S4B), in accordance with our in vitro data (Fig. S3C). When tumors reached 2.0 cm in diameter, we harvested soft organs (ovaries, spleen, kidneys, liver, brain, and lungs) and bones for *ex vivo* IVIS-imaging to quantify metastasis. We found that 6 of the 8 mice (75%) implanted with MCF10A-PIK3CA^{H1047R} showed metastases in distant organs (Fig. 3C), which was confirmed by H&E (Fig. S4C), while none of the 4 mice implanted with MCF10A-PIK3CA^{H1047R}/STAT5a^{ca} had a detectable metastatic signal in any organ (Fig. 3C, 3D). To determine the stage at which STAT5 influences metastasis, we tail vein-injected MCF10A-PIK3CA^{H1047R} cells and MCF10A-PIK3CA^{H1047R}/STAT5a^{ca} cells into NSG mice, and compared the mice for pulmonary

metastatic burden over a window of 6 weeks by *in vivo* IVIS imaging. As shown in Fig. 3E and 3F, the two groups developed lung metastasis overtime without discernable differences, suggesting that STAT5a does not significantly impact metastatic development after intravasation. Taken together, these *in vitro* and *in vivo* results indicate that STAT5 activation restricts metastatic potential of human breast cancer cells primarily by suppressing local migration, invasion and possibly intravasation.

High *STAT5A* level predicts favorable outcome in breast cancer patients

By immunohistochemical staining of breast cancer specimens, STAT5 activation has been correlated with ER+ breast cancer with a more favorable prognosis [10, 11], but this potential biomarker has not been studied in large public datasets or within specific breast cancer subtypes. Therefore, to further explore the prognostic potential of STAT5 in breast cancer patients, we performed bioinformatic analyses to compare outcome of patients bearing *STAT5*-low vs. *STAT5*-high breast tumors in two publicly available datasets. Due to the scarcity of STAT5 and pSTAT5 protein data in public datasets, we compared tumors with high vs. low mRNA levels of *STAT5A* (which has Spearman correlation of 0.37 with STAT5A protein levels in TCGA based on LinkedOmics [36]). In the EMC-MSK dataset [37, 38], we found that higher *STAT5A* mRNA levels were correlated with a better metastasis-free survival when all patients were included ($p = 0.0251$; Fig. 3G). When the patients were separated into ERα+, HER2+ and TNBC subtypes, the association was highly significant among the ERα+ breast cancer patients but was not detected in HER2+ patients or triple-negative patients (Fig. S5A). Consistent with the finding, in the METABRIC Database [39, 40], higher *STAT5A* expression was associated with better relapse-free survival among all breast cancer patients (Fig. 3H), and also in Luminal A, and Luminal B patients, but not among other subtypes (Fig. S5B). In addition, higher *STAT5A* expression was associated with better overall survival among all breast cancer patients in METABRIC Database (Fig. 3I),

As a transcription factor, STAT5 potentially regulates expression of multiple genes in breast tumors. Therefore, we next asked whether a STAT5 gene expression signature is correlated with patient outcome. While a STAT5-dependent gene set in the normal mouse mammary gland has been reported [41], a STAT5 gene signature in human breast cancer cells is not yet available. We performed RNAseq on a panel of human breast cancer cell lines carrying vector vs. lenti-STAT5a^{ca}, and generated a STAT5A gene signature consisting of 105 genes that are upregulated in any 4 out of 6 pairs (Supplementary Table 1). This STAT5A signature exhibited a significant correlation with *STAT5A* mRNA levels in METABRIC and TCGA breast cancer datasets (Fig. S6A, S6B). In the TCGA dataset, higher STAT5A signature scores were associated with better disease-free survival, although *STAT5A* mRNA levels were not associated with disease-free survival (Fig. S6A). Likewise, in the METABRIC dataset, this gene signature was associated with better relapse-free survival although it lacked power to correlate with outcome in breast cancer subtypes (Fig. S6C). Since EMC-MSK dataset is based on Microarray and does not include many of the genes in our signature, we did not attempt correlation analysis. Together, these bioinformatic data indicate that *STAT5* expression levels and activity can serve as a biomarker for favorable prognosis for breast cancer patients, especially patients with ERα+ breast cancer. However,

the power of prediction is relatively modest, and STAT5a mRNA and its gene signature do not always agree possibly due to several reasons, including uncertain correlation between STAT5a gene expression levels and protein activity levels (which the gene signature) and potential contributions of STAT5b and other STAT family members to the gene signature levels in patients.

STAT5a alters protein levels that regulate epithelial-mesenchymal transition (EMT)

To gain insight into mechanisms by which STAT5 activation blocks breast cancer metastasis, we used the reverse-phase protein array (RPPA) to identify proteins expressed differentially between murine mammary tumors initiated by *PIK3CA*^{H1047R} vs. *PIK3CA*^{H1047R}/*Stat5a*^{ca}. Among 243 antibodies detecting total and phosphorylated proteins, 90 were different between these two groups of tumors (Fig. S7). The top 4 down-regulated proteins in the PIK3CA^{H1047R} /STAT5a^{ca} tumor cohort include a prominent EMT driver, Slug (SNAI2) and a key EMT marker, Vimentin (VIM) (Fig. 4A). We confirmed by Western blotting that STAT5a^{ca} suppressed these two proteins, and we also detected decreased levels of another EMT regulator, ZEB1 and the mesenchymal marker N-cadherin (CDH2), as well as increased levels of the epithelial marker E-cadherin (CDH1) and the milk protein β-casein in murine mammary tumors (Fig. 4B). We validated these data in human breast cancer cells by comparing MCF10A-PIK3CA^{H1047R} cells vs. MCF10A-PIK3CA^{H1047R}/STAT5a^{ca} cells (Fig. 4C), and we additionally detected STAT5a-mediated suppression of two more EMT regulators, Snail (SNAI1) and TWIST (Fig. 4C), consistent with previous studies in cell cultures [19].

To determine if STAT5 regulates the transcription of these genes, we first performed real-time PCR on these human cancer cells. Consistent with the findings in proteins, mRNA levels of *CDH2*, *VIM*, *SNAI1*, *SNAI2*, *TWIST1* and *ZEB1* were decreased by STAT5a^{ca}, but *CDH1* and *ZEB2* were not affected (Fig. 4D). Interestingly, we also found an increase of miR200c, a microRNA which was reported to suppress the EMT programs via a ZEB/miR-200 feedback loop [42]. Importantly, the analysis of published ChIPseq data comparing mammary gland cells with different gene dosages of *Stat5a* and *Stat5b* at lactation day 1 [43] revealed that multiple EMT-related genes, including *Vim* and *Zeb1, Zeb2*, had STAT5 bound to their promoters or gene bodies (Fig. 4E, S8, S9), suggesting that STAT5 may regulate EMT via transactivation of EMT regulators.

This study using multiple in vivo models as well as multiple cell lines demonstrates a dichotomous role of STAT5 in cancer initial development and subsequent metastasis (Fig. 4F). We previously published that STAT5 accelerates precancerous lesion progression by lowering the apoptosis anti-cancer barrier (without a significant impact on cell proliferation) [8, 44]. The data presented in this study further strength this previous finding and show a diminished impact of STAT5 on growth of established breast tumor cells especially if PIK3CA is activated. On the other hand, our ErbB2 and PIK3CA mouse model data demonstrate that STAT5 also programs precancerous and cancerous cells into a functionally differentiated state that is characterized by the expression of alveolar markers and milk proteins (Fig. 1, 2). These data provide *in vivo* support to previous reports of JAK2-STAT5 signaling in promoting alveolar differentiation of cultured breast cancer cells [18, 19].

Of note, it remains to be determined whether the gain of these alveolar features truly caused these precancerous cells to gain or lose stem/progenitor properties compared to other precancerous cells that did not acquire STAT5 activation. It has been reported that certain alveolar cells marked by the expression of the whey acidic protein gene, a transcriptional target of STAT5, can gain multipotency following a reproductive cycle [45, 46], and that they are probably the cells of origin of tumors in mice transgenic for ErbB2 [47].

Using both *in vitro* and *in vivo* experiments, we further demonstrate that STAT5 suppresses EMT and restrains early steps of metastasis including migration and invasion although exerting no significant impact on tumor cells that have already disseminated (Fig 3). It is conceivable that a more differentiated epithelial state may counter EMT activators and hinder migration, invasion, and metastasis, but it remains to be determined how much functional differentiation per se contributes to blocked metastasis. Furthermore, while STAT5 regulates multiple EMT-related genes likely via transcriptional activation (Fig. 4), the crucial EMT regulators directly controlled by STAT5 remain to be elucidated. In addition, as multiple previous studies have reported STAT5's promotion of EMT and metastasis [20, 21, 23–26], the molecular mechanism for these apparently opposing roles of STAT5 on EMT in different tissue contexts remains to be investigated.

In conclusion, while it promotes breast cancer formation at least partly by suppressing the apoptosis anticancer barrier and may be a chemoprevention target [8, 44], STAT5 activation initiates a lactogenic network in precancerous and cancerous cells, suppresses EMT, and impairs cancer migration, invasion, and dissemination to distant organs, consequently serving as a potential biomarker in breast cancer prognosis (Fig. 4F).

MATERIAL AND METHODS

Animals

Wild-type FVB/N mice and MMTV-tva transgenic mice (on the FVB background) were bred in house. NOD.Cg-Prkdc scid Il2rg tm1Wjl /SzJ (NSG) mice were purchased from the Jackson lab (Bar Harbor, ME, USA). The animal experimentation protocol was approved by the BCM institutional Animal Care and Use Committee, and conducted under the guidelines described in the NIH Guide for the Care and Use of Laboratory Animals.

Virus production and titration

The plasmid RCAS-HA-*ErbB2*^{ca} carrying the HA-tagged constitutively activated *ErbB2* mutant gene was reported in our previous work [27]. The plasmid RCAS-FLAG-*Stat5a*^{ca} [6] carries the FLAG-tagged activated mutant of *STAT5a*, which was subcloned from the pMX-Stat5a1*6 [48]. The plasmid FUCGW-*PIK3CA*^{H1047R} [33] carries a constitutively active mutant of *PIK3CA* along with a GFP marker. The plasmid FUW-*Stat5a*^{ca} was constructed by subcloning *Stat5a*1*6 to the FUW vector and adding a mCherry cassette by infusion cloning. The production and titration for both avian retrovirus and lentivirus were performed as described before [27, 49, 50]. All mice were randomized at the time of experiments.

Mouse tumor model generation

Virus and breast cells were delivered into mouse mammary glands by intraductal injection as previously described [50–52]. To generate HER2+ mammary precancerous lesions and tumors, 10-week-old MMTV-*tva* (MA) female mice were intraductally injected via the #4 teat with RCAS-HA-*ErbB2*^{ca} (5×10^4 IUs per gland) alone or together with RCAS-FLAG-*Stat5a*^{ca} (10^7 IUs per gland). The injected mammary glands were harvested 2 weeks after virus injection for precancerous lesion studies. Tumors were scored when the diameter reached ~2-3mm and can be detected by palpation. The length and width of tumors were measured with a caliper twice per week until the tumor size reached the ethical endpoint (1.5-2 cm). To generate ER+ mammary tumors, 10-week-old female mice in FVB/N background were intraductally injected with FUCGW-*PIK3CA*^{H1047R} (10^7 IUs per gland) alone or together with FUW-FLAG-*Stat5a*^{ca} (7×10^7 IUs per gland). For the spontaneous metastasis model, 10-week-old NSG mice were intraductally implanted with luciferase-tagged MCF10A-PIK3CA^{H1047R} cells or MCF10A-PIK3CA^{H1047R}/STAT5a^{ca} cells (30 000 cells per gland). The lesion burden was determined biweekly by bioluminescence for 16 weeks post cell implantation when >50% of mice developed palpable tumors. The metastasis burden across organs was determined by bioluminescence at harvest. For the experimental metastasis model, these two groups of cells were tail vein-injected into 10-week-old NSG mice (1×10^6 cells per mouse). The metastasis burden was determined weekly by bioluminescence for 6 weeks following tail vein injection.

Cell culture and stable line generation

Breast MCF10A sublines stably expressing *PIK3CA*^{H1047R} and/or *Stat5a*^{ca} were generated by transducing luciferase-tagged cells with lentiviruses carrying FUCGW-*PIK3CA*^{H1047R} [33] or matched vector FUCGW and/or FUW-*Stat5a*^{ca}-mCherry or matched vector FUW-mCherry. In brief, cells were incubated with viral particles (M.O.I.=10) and 10 μg/mL polybrene, centrifuged at 1 100 xg for 30 min at 37°C, and washed with PBS. After passage, cells were FACS-sorted for GFP and/or mCherry. 3D culture assay was performed as published [53]. In brief, 5 000 MCF10A cells in media containing 2% growth factor-reduced Matrigel (BD Biosciences, Franklin Lakes, NJ, USA) were plated to 8-well chamber slides precoated with a base layer of 100% Matrigel. 3D growth was imaged at day 4 and day 7. Breast cancer cell lines MCF7, BT20, MDA-MB-231, T47D were transduced with FUW-*Stat5a*^{ca}-mCherry or matched vector FUW-mCherry and FACS-sorted to derive sublines.

Immunohistochemistry (IHC) and immunofluorescence (IF)

Immunochemistry staining was performed using the Vectastain Elite ABC system (Vector Laboratories, Burlingame, CA, USA) and developed using DAB as chromogen (Agilent Dako, Santa Clara, CA, USA). The antibodies used in this study include anti-HA (#3724, 1:4 000, Cell Signaling Technology, Danvers, MA, USA), anti-FLAG (#8146, 1:400, Cell Signaling Technology), anti-β-casein (sc-166530, 1:600, Santa Cruz Biotechnology, Dallas, TX, USA), and anti-BCL-xL (sc-8044, 1:200, Santa Cruz Biotechnology). For IF staining, the anti-PLIN2 (NB110-40877, 1:600, Novus Biologicals, Littleton, CO, USA) primary antibody was used. Sections were incubated with primary antibodies overnight at 4°C, followed by 30 min incubation with Alexa Fluor 568-conjugated anti-rabbit

antibodies (#A11011, 1:200, Invitrogen, Waltham, MA, USA). The slides were mounted with VECTASHIELD Antifade Mounting Medium with DAPI (Vector Laboratories).

Western blotting

Murine tumors were ground in a mortar with liquid N_2, and proteins were extracted in lysis buffer (MPER) containing protease inhibitor. Proteins from MCF10A and MCF7 were extracted by cell lysis in RIPA buffer (Bio-Rad, Hercules, CA, USA). 30 to 50 μg of protein per lane were separated in SDS-PAGE and transferred onto nitrocellulose membrane (Bio-Rad) for incubation with antibodies and detection using an ECL chemiluminescent kit (ProteinSimple, San Jose, CA, USA). The antibodies used include antibodies against BCL-2 (sc-7382, 1:1 000, Santa Cruz Biotechnology), BCL-xL (#sc-8044, 1:1 000, Santa Cruz Biotechnology), E-cadherin (Cell Signaling Technology, #3195, 1:1 000), N-cadherin (#610920, 1:1 000, BD Biosciences), Vimentin (#5741, 1:1 000, Cell Signaling Technology), Snail (#3879, 1:1 000, Cell Signaling Technology), Slug (#9585, 1:1 000, Cell Signaling Technology), FLAG (#8146, 1:1 000, Cell Signaling Technology), β-casein (#MA1-46056, 1:1 000, Invitrogen), TWIST (#sc-81417, 1:1 000, Santa Cruz Biotechnology), ZEB1 (#70512, 1:1 000, Cell Signaling Technology), and β-actin (#A5441, 1:5 000, Sigma-Aldrich, St. Louis, MO, USA). At least three independent biological repeats were performed.

Transwell migration and invasion assay

Transwell migration and invasion assays were performed as we described previously [54]. The MCF-10A cells were seeded at 20 000 cells per well and incubated 16 hours for migration assay or seeded at 50 000 cells per well for 20 hours for invasion assay. MCF-7 cells were seeded at 50 000 cells and incubated for 16 hours for migration assays and 100 000 cells per well for 48 hours for invasion assays. At least three independent experiments were performed.

Reverse phase protein array (RPPA) analysis

Reverse phase protein array assays were carried out as reported previously [55]. Protein lysates were prepared from tumors with modified tissue protein extraction reagent (TPER; Pierce, Thermo Scientific, Appleton, WI, USA) and a cocktail of protease and phosphatase inhibitors. Then 243 antibodies against total or phosphorylated protein were used. The full list of antibodies is at https://www.bcm.edu/centers/cancer-center/research/shared-resources/cprit-cancer-proteomics-and-metabolomics/reverse-phase-proteinarray.

Real-time PCR

Cells were lysed with TRI Reagent (Sigma-Aldrich). Total RNA was purified from cells using Direct-zol RNA Microprep Kit (Zymo Research, Irvine, CA, USA). cDNA synthesis from mRNA was carried out using a SuperScript III First-Strand Synthesis System (Invitrogen), and Takyo No Rox SYBR MasterMix dTTP Blue (Eurogentec, Fremont, CA, USA) was used for real-time PCR assay. For microRNA, the miRCURY LNA miRNA PCR Starter Kit (QIAGEN, Germantown, MD, USA) was used to construct cDNA and also real-time PCR assay. All qPCR assays were conducted in a CFX96 qPCR Instrument

(Bio-Rad). Four independent repeats were performed. mRNA was normalized to human acidic ribosomal protein (hARP). miR-200c was normalized to miR-103a. The primers used for the PCR are:

CDH1: 5'-CAGGTCTCCTCTTGGCTCTG-3' and 5'-GACCGGTGCAATCTTCAAAA-3'; *CDH2*: 5'-GTGCATGAAGGACAGCCTCT-3' and 5'-AGCTTCTCACGGCATACACC-3'; *VIM*: 5'-CGAAAACACCCTGCAATCTT-3' and 5'-CTGGATTTCCTCTTCGTGGA-3'; *SNAI1*: 5'-CTTCTCTAGGCCCTGGCTG-3' and 5'-CATCTGAGTGGGTCTGGAGG-3'; *SNAI2*: 5'-TCGGACCCACACATTACCTT-3' and 5'-TGACCTGTCTGCAAATGCTC-3'; *TWIST1:* 5'-GGACAAGCTGAGCAAGATTCA-3' and 5'-CGGAGAAGGCGTAGCTGAG-3'; *ZEB1*: 5'-AGCAGTGAAAGAGAAGGGAATGC-3' and 5'-GGTCCTCTTCAGGTGCCTCAG-3'; *ZEB2*: 5'-TTTCAGGGAGAATTGCTTGA-3' and 5'-CACATGCATACATGCCACTC-3'; hARP: 5'-CACCATTGAAATCCTGAGTGATGT-3' and 5'-TGACCAGCCCAAAGGAGAAG -3'.

Bioinformatic studies of clinical data from public datasets, ChIPseq data study, and statistical analyses

Clinical data were collected from the Erasmus Medical Center/Memorial Sloan-Kettering (EMC-MSK) dataset [37, 38], the METABRIC dataset [39, 40] and the TCGA dataset [56, 57]. To generate STAT5A signature, we built 6 pairs of human breast and cancer cell lines with or without $STAT5a^{ca}$ overexpression (MCF10A, $MCF10A\text{-}PIK3CA^{H1047R}$, MCF7, BT20, MDA-MB-231, T47D) for RNAseq analysis (Novogene, China), and fold change of gene expression was calculated based on the ratio of fpkm values in $STAT5a^{ca}$ overexpressed samples vs vector controls. We generated a STAT5A gene signature consisting of 105 genes that were induced over 2-fold by $STAT5a^{ca}$ overexpression in at least 4 of the 6 cell lines and calculated STAT5A gene signature scores using z-score method. Survival R package was used to compare Kaplan-Meier survival curves using the log rank test.

ChIPseq data of STAT5 sequentially knockout mice at lactation day 1 were previously published [43]. The EMT-related gene list is derived from EMTome by Vasaikar et al [58]. Raw public data were downloaded with accession number GSE37646 and GSE40930. STAT5A ChIPseq raw data (GSE40930) were mapped to mm10 with BWA (0.7.4). We called significant peaks using MACS2 (2.2.7.1) with default parameters. To find out EMT genes bound by STAT5A, bedtools (2.28.0) was applied to intersect significant peak regions and gene promoters or gene bodies. We utilized deeptools (3.5.1) to generate normalized bigwig files from bam files with RPGC normalization method. RNA-seq data (GSE37646) were mapped to mm10 using STAR (2.5.2b) and then counted using HTSeq (2.7).

For tumor growth of HER2+ tumors, Kaplan-Meier survival curves were analyzed by Prism 9, and *P* values were calculated using the log-rank test. For assessment of spontaneous metastasis, the *P* value was calculated by Fisher's exact test. A two-tailed Student's *t* test was applied for all other experiments. Results are expressed as the mean ±SD.

Supplementary Material

Refer to Web version on PubMed Central for supplementary material.

Acknowledgements

This work was supported by DOD CDMRP BC191649 & BC191646 (to Y.L.). The authors thank the SPORE-funded (P50CA186784) Pathology Core Facility at the Breast Center for tissue processing and Dr. Gary Chamness for helpful comments on the manuscript; the Cytometry and Cell Sorting Core at Baylor College of Medicine with funding from the CPRIT Core Facility Support Award (CPRIT-RP180672), the NIH (P30 CA125123 and S10 RR024574) and the expert assistance of Joel M. Sederstrom; the Antibody-Based Proteomics Core (RPPA core) at Baylor College of Medicine funded by CPRIT Core Facility Award (RP210227) and P30 Cancer Center Support Grant (NCI-CA125123), NIH S10 instrument award (S10OD028648-01), and the expert help of Dr. Xuan Wang. The authors thank Le Ma for gifting reagents and Dr. Wen Bu for intellectual input. ML is supported by the Chinese Scholarship Council (CSC), AK was supported by T32-CA203690. JMR is supported by NIH016303. CJC is supported by NIH CA125123.

Availability of data and materials

Available upon request to liyi@bcm.edu.

Reference

1. Salas A, Hernandez-Rocha C, Duijvestein M, Faubion W, McGovern D, Vermeire S et al. JAK-STAT pathway targeting for the treatment of inflammatory bowel disease. Nature reviews Gastroenterology & hepatology 2020.
2. Haricharan S, Li Y. STAT signaling in mammary gland differentiation, cell survival and tumorigenesis. Molecular and cellular endocrinology 2014; 382: 560–569. [PubMed: 23541951]
3. Hennighausen L, Robinson GW. Interpretation of cytokine signaling through the transcription factors STAT5A and STAT5B. Genes & development 2008; 22: 711–721. [PubMed: 18347089]
4. Wagner KU, Rui H. Jak2/Stat5 signaling in mammogenesis, breast cancer initiation and progression. J Mammary Gland Biol Neoplasia 2008; 13: 93–103. [PubMed: 18228120]
5. Watson CJ, Neoh K. The Stat family of transcription factors have diverse roles in mammary gland development. Seminars in cell & developmental biology 2008; 19: 401–406. [PubMed: 18723104]
6. Dong J, Tong T, Reynado AM, Rosen JM, Huang S, Li Y. Genetic manipulation of individual somatic mammary cells in vivo reveals a master role of STAT5a in inducing alveolar fate commitment and lactogenesis even in the absence of ovarian hormones. Dev Biol 2010; 346: 196–203. [PubMed: 20691178]
7. Shi A, Dong J, Hilsenbeck S, Bi L, Zhang H, Li Y. The Status of STAT3 and STAT5 in Human Breast Atypical Ductal Hyperplasia. PLoS One 2015; 10: e0132214. [PubMed: 26146825]
8. Haricharan S, Dong J, Hein S, Reddy JP, Du Z, Toneff M et al. Mechanism and preclinical prevention of increased breast cancer risk caused by pregnancy. Elife 2013; 2: e00996. [PubMed: 24381245]
9. Cotarla I, Ren S, Zhang Y, Gehan E, Singh B, Furth PA. Stat5a is tyrosine phosphorylated and nuclear localized in a high proportion of human breast cancers. Int J Cancer 2004; 108: 665–671. [PubMed: 14696092]
10. Nevalainen MT, Xie J, Torhorst J, Bubendorf L, Haas P, Kononen J et al. Signal transducer and activator of transcription-5 activation and breast cancer prognosis. Journal of clinical oncology : official journal of the American Society of Clinical Oncology 2004; 22: 2053–2060. [PubMed: 15169792]
11. Peck AR, Witkiewicz AK, Liu C, Stringer GA, Klimowicz AC, Pequignot E et al. Loss of nuclear localized and tyrosine phosphorylated Stat5 in breast cancer predicts poor clinical outcome and increased risk of antiestrogen therapy failure. Journal of clinical oncology : official journal of the American Society of Clinical Oncology 2011; 29: 2448–2458. [PubMed: 21576635]

12. Iavnilovitch E, Cardiff RD, Groner B, Barash I. Deregulation of Stat5 expression and activation causes mammary tumors in transgenic mice. Int J Cancer 2004; 112: 607–619. [PubMed: 15382041]

13. Iavnilovitch E, Eilon T, Groner B, Barash I. Expression of a carboxy terminally truncated Stat5 with no transactivation domain in the mammary glands of transgenic mice inhibits cell proliferation during pregnancy, delays onset of milk secretion, and induces apoptosis upon involution. Molecular reproduction and development 2006; 73: 841–849. [PubMed: 16596634]

14. Eilon T, Groner B, Barash I. Tumors caused by overexpression and forced activation of Stat5 in mammary epithelial cells of transgenic mice are parity-dependent and developed in aged, postestropausal females. Int J Cancer 2007; 121: 1892–1902. [PubMed: 17640063]

15. Yamashita H, Nishio M, Ando Y, Zhang Z, Hamaguchi M, Mita K et al. Stat5 expression predicts response to endocrine therapy and improves survival in estrogen receptor-positive breast cancer. Endocrine-related cancer 2006; 13: 885–893. [PubMed: 16954437]

16. Strauss BL, Bratthauer GL, Tavassoli FA. STAT 5a expression in the breast is maintained in secretory carcinoma, in contrast to other histologic types. Human pathology 2006; 37: 586–592. [PubMed: 16647957]

17. Nouhi Z, Chughtai N, Hartley S, Cocolakis E, Lebrun JJ, Ali S. Defining the role of prolactin as an invasion suppressor hormone in breast cancer cells. Cancer Res 2006; 66: 1824–1832. [PubMed: 16452244]

18. Sultan AS, Xie J, LeBaron MJ, Ealley EL, Nevalainen MT, Rui H. Stat5 promotes homotypic adhesion and inhibits invasive characteristics of human breast cancer cells. Oncogene 2005; 24: 746–760. [PubMed: 15592524]

19. Sultan AS, Brim H, Sherif ZA. Co-overexpression of Janus kinase 2 and signal transducer and activator of transcription 5a promotes differentiation of mammary cancer cells through reversal of epithelial-mesenchymal transition. Cancer science 2008; 99: 272–279. [PubMed: 18271926]

20. Wang J, Rouse C, Jasper JS, Pendergast AM. ABL kinases promote breast cancer osteolytic metastasis by modulating tumor-bone interactions through TAZ and STAT5 signaling. Sci Signal 2016; 9: ra12. [PubMed: 26838548]

21. Gu L, Vogiatzi P, Puhr M, Dagvadorj A, Lutz J, Ryder A et al. Stat5 promotes metastatic behavior of human prostate cancer cells in vitro and in vivo. Endocrine-related cancer 2010; 17: 481–493. [PubMed: 20233708]

22. Li H, Zhang Y, Glass A, Zellweger T, Gehan E, Bubendorf L et al. Activation of signal transducer and activator of transcription-5 in prostate cancer predicts early recurrence. Clin Cancer Res 2005; 11: 5863–5868. [PubMed: 16115927]

23. Lee TK, Man K, Poon RT, Lo CM, Yuen AP, Ng IO et al. Signal transducers and activators of transcription 5b activation enhances hepatocellular carcinoma aggressiveness through induction of epithelial-mesenchymal transition. Cancer Res 2006; 66: 9948–9956. [PubMed: 17047057]

24. Koppikar P, Lui VW, Man D, Xi S, Chai RL, Nelson E et al. Constitutive activation of signal transducer and activator of transcription 5 contributes to tumor growth, epithelial-mesenchymal transition, and resistance to epidermal growth factor receptor targeting. Clin Cancer Res 2008; 14: 7682–7690. [PubMed: 19047094]

25. Talati PG, Gu L, Ellsworth EM, Girondo MA, Trerotola M, Hoang DT et al. Jak2-Stat5a/b Signaling Induces Epithelial-to-Mesenchymal Transition and Stem-Like Cell Properties in Prostate Cancer. The American journal of pathology 2015; 185: 2505–2522. [PubMed: 26362718]

26. Kinslechner K, Schorghofer D, Schutz B, Vallianou M, Wingelhofer B, Mikulits W et al. Malignant Phenotypes in Metastatic Melanoma are Governed by SR-BI and its Association with Glycosylation and STAT5 Activation. Molecular cancer research : MCR 2018; 16: 135–146. [PubMed: 28974560]

27. Du Z, Podsypanina K, Huang S, McGrath A, Toneff MJ, Bogoslovskaia E et al. Introduction of oncogenes into mammary glands in vivo with an avian retroviral vector initiates and promotes carcinogenesis in mouse models. Proceedings of the National Academy of Sciences of the United States of America 2006; 103: 17396–17401. [PubMed: 17090666]

28. Liu X, Robinson GW, Wagner KU, Garrett L, Wynshaw-Boris A, Hennighausen L. Stat5a is mandatory for adult mammary gland development and lactogenesis. Genes & development 1997; 11: 179–186. [PubMed: 9009201]
29. Dumon S, Santos SC, Debierre-Grockiego F, Gouilleux-Gruart V, Cocault L, Boucheron C et al. IL-3 dependent regulation of Bcl-xL gene expression by STAT5 in a bone marrow derived cell line. Oncogene 1999; 18: 4191–4199. [PubMed: 10435632]
30. Minieri V, De Dominici M, Porazzi P, Mariani SA, Spinelli O, Rambaldi A et al. Targeting STAT5 or STAT5-Regulated Pathways Suppresses Leukemogenesis of Ph+ Acute Lymphoblastic Leukemia. Cancer Res 2018; 78: 5793–5807. [PubMed: 30154155]
31. Schorr K, Furth PA. Induction of bcl-xL expression in mammary epithelial cells is glucocorticoid-dependent but not signal transducer and activator of transcription 5-dependent. Cancer Res 2000; 60: 5950–5953. [PubMed: 11085510]
32. Cancer Genome Atlas N. Comprehensive molecular portraits of human breast tumours. Nature 2012; 490: 61–70. [PubMed: 23000897]
33. Young A, Bu W, Jiang W, Ku A, Kapali J, Dhamne S et al. Targeting the Pro-survival Protein BCL-2 to Prevent Breast Cancer. Cancer prevention research 2022; 15: 3–10. [PubMed: 34667127]
34. Meyer DS, Brinkhaus H, Muller U, Muller M, Cardiff RD, Bentires-Alj M. Luminal expression of PIK3CA mutant H1047R in the mammary gland induces heterogeneous tumors. Cancer Res 2011; 71: 4344–4351. [PubMed: 21482677]
35. Liu P, Cheng H, Santiago S, Raeder M, Zhang F, Isabella A et al. Oncogenic PIK3CA-driven mammary tumors frequently recur via PI3K pathway-dependent and PI3K pathway-independent mechanisms. Nature medicine 2011; 17: 1116–1120.
36. Vasaikar SV, Straub P, Wang J, Zhang B. LinkedOmics: analyzing multi-omics data within and across 32 cancer types. Nucleic acids research 2018; 46: D956–D963. [PubMed: 29136207]
37. Zhang XH, Wang Q, Gerald W, Hudis CA, Norton L, Smid M et al. Latent bone metastasis in breast cancer tied to Src-dependent survival signals. Cancer Cell 2009; 16: 67–78. [PubMed: 19573813]
38. Zhang XH, Jin X, Malladi S, Zou Y, Wen YH, Brogi E et al. Selection of bone metastasis seeds by mesenchymal signals in the primary tumor stroma. Cell 2013; 154: 1060–1073. [PubMed: 23993096]
39. Curtis C, Shah SP, Chin SF, Turashvili G, Rueda OM, Dunning MJ et al. The genomic and transcriptomic architecture of 2,000 breast tumours reveals novel subgroups. Nature 2012; 486: 346–352. [PubMed: 22522925]
40. Pereira B, Chin SF, Rueda OM, Vollan HK, Provenzano E, Bardwell HA et al. The somatic mutation profiles of 2,433 breast cancers refines their genomic and transcriptomic landscapes. Nature communications 2016; 7: 11479.
41. Metser G, Shin HY, Wang C, Yoo KH, Oh S, Villarino AV et al. An autoregulatory enhancer controls mammary-specific STAT5 functions. Nucleic acids research 2016; 44: 1052–1063. [PubMed: 26446995]
42. Hill L, Browne G, Tulchinsky E. ZEB/miR-200 feedback loop: at the crossroads of signal transduction in cancer. Int J Cancer 2013; 132: 745–754. [PubMed: 22753312]
43. Yamaji D, Kang K, Robinson GW, Hennighausen L. Sequential activation of genetic programs in mouse mammary epithelium during pregnancy depends on STAT5A/B concentration. Nucleic acids research 2013; 41: 1622–1636. [PubMed: 23275557]
44. Johnston AN, Bu W, Hein S, Garcia S, Camacho L, Xue L et al. Hyperprolactinemia-inducing antipsychotics increase breast cancer risk by activating JAK-STAT5 in precancerous lesions. Breast cancer research : BCR 2018; 20: 42. [PubMed: 29778097]
45. Wagner KU, Boulanger CA, Henry MD, Sgagias M, Hennighausen L, Smith GH. An adjunct mammary epithelial cell population in parous females: its role in functional adaptation and tissue renewal. Development 2002; 129: 1377–1386. [PubMed: 11880347]
46. Matulka LA, Triplett AA, Wagner KU. Parity-induced mammary epithelial cells are multipotent and express cell surface markers associated with stem cells. Developmental biology 2007; 303: 29–44. [PubMed: 17222404]

47. Henry MD, Triplett AA, Oh KB, Smith GH, Wagner KU. Parity-induced mammary epithelial cells facilitate tumorigenesis in MMTV-neu transgenic mice. Oncogene 2004; 23: 6980–6985. [PubMed: 15286714]

48. Onishi M, Nosaka T, Misawa K, Mui AL, Gorman D, McMahon M et al. Identification and characterization of a constitutively active STAT5 mutant that promotes cell proliferation. Mol Cell Biol 1998; 18: 3871–3879. [PubMed: 9632771]

49. Bu W, Li Y. Intraductal Injection of Lentivirus Vectors for Stably Introducing Genes into Rat Mammary Epithelial Cells in Vivo. J Mammary Gland Biol Neoplasia 2020; 25: 389–396. [PubMed: 33165800]

50. Bu W, Xin L, Toneff M, Li L, Li Y. Lentivirus vectors for stably introducing genes into mammary epithelial cells in vivo. J Mammary Gland Biol Neoplasia 2009; 14: 401–404. [PubMed: 19936990]

51. Behbod F, Kittrell FS, Lamarca H, Edwards D, Kerbawy S, Heestand JC et al. An intraductal human-in-mouse transplantation model mimics the subtypes of ductal carcinoma in situ. Breast cancer research : BCR 2009; 11: R66. [PubMed: 19735549]

52. Reddy JP, Li Y. The RCAS-TVA system for introduction of oncogenes into selected somatic mammary epithelial cells in vivo. J Mammary Gland Biol Neoplasia 2009; 14: 405–409. [PubMed: 19936988]

53. Debnath J, Muthuswamy SK, Brugge JS. Morphogenesis and oncogenesis of MCF-10A mammary epithelial acini grown in three-dimensional basement membrane cultures. Methods 2003; 30: 256–268. [PubMed: 12798140]

54. Yue F, Jiang W, Ku AT, Young AIJ, Zhang W, Souto EP et al. A Wnt-Independent LGR4-EGFR Signaling Axis in Cancer Metastasis. Cancer Res 2021; 81: 4441–4454. [PubMed: 34099494]

55. Creighton CJ, Huang S. Reverse phase protein arrays in signaling pathways: a data integration perspective. Drug design, development and therapy 2015; 9: 3519–3527. [PubMed: 26185419]

56. Comprehensive molecular portraits of human breast tumours. Nature 2012; 490: 61–70. [PubMed: 23000897]

57. Ciriello G, Gatza ML, Beck AH, Wilkerson MD, Rhie SK, Pastore A et al. Comprehensive Molecular Portraits of Invasive Lobular Breast Cancer. Cell 2015; 163: 506–519. [PubMed: 26451490]

58. Vasaikar SV, Deshmukh AP, den Hollander P, Addanki S, Kuburich NA, Kudaravalli S et al. EMTome: a resource for pan-cancer analysis of epithelial-mesenchymal transition genes and signatures. British journal of cancer 2021; 124: 259–269. [PubMed: 33299129]

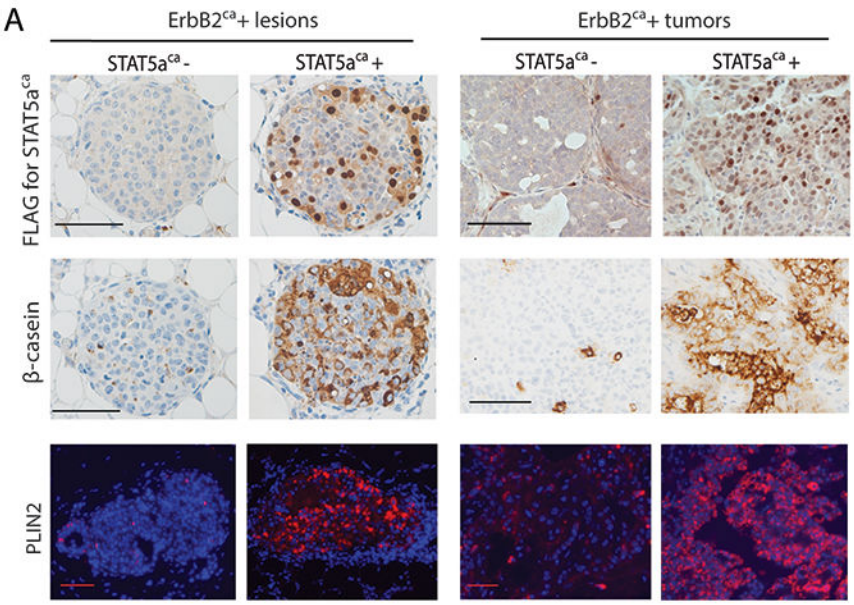

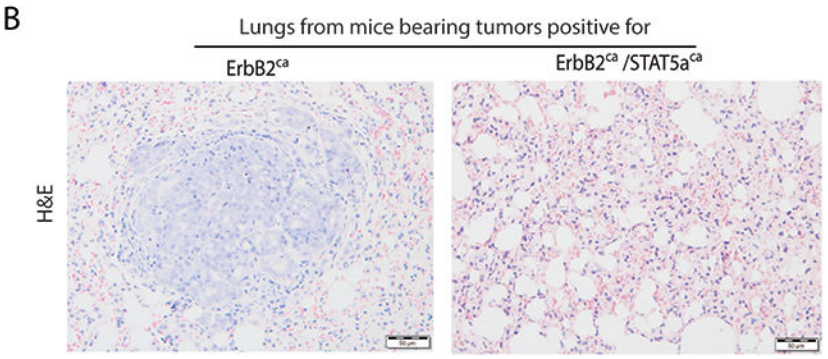

C

Metastasis	Mice bearing tumors positive for		P-value
	ErbB2ca	ErbB2ca /STAT5aca	
+	12	1	0.018
-	18	15	

Figure 1. STAT5a^{ca} causes lactogenic differentiation in *ErbB2^{ca}*-induced precancerous lesions and tumors, and it blocks lung metastases.

(A) Representative images of immunochemistry (IHC) staining for FLAG in STAT5a^{ca} and two milk production markers, β-casein and PLIN2, in precancerous lesions and tumors. Scale bars: 50 μm. N = 5 for tumor comparison; N = 7 for precancerous lesion comparison. (B) H&E images of a pulmonary metastatic nodule from a *ErbB2^{ca}*-initiated primary tumor and a benign lung from a mouse bearing a *ErbB2^{ca}/STAT5a^{ca}* primary tumor. Scale bars: 50 μm.

(C) Summary of the lung metastatic incidence in mice infected by RCAS-*ErbB2*^{ca} alone and in mice bearing ErbB2^{ca}+/STAT5a^{ca}+ tumors. The Fisher's exact test was used and $*P < 0.05$.

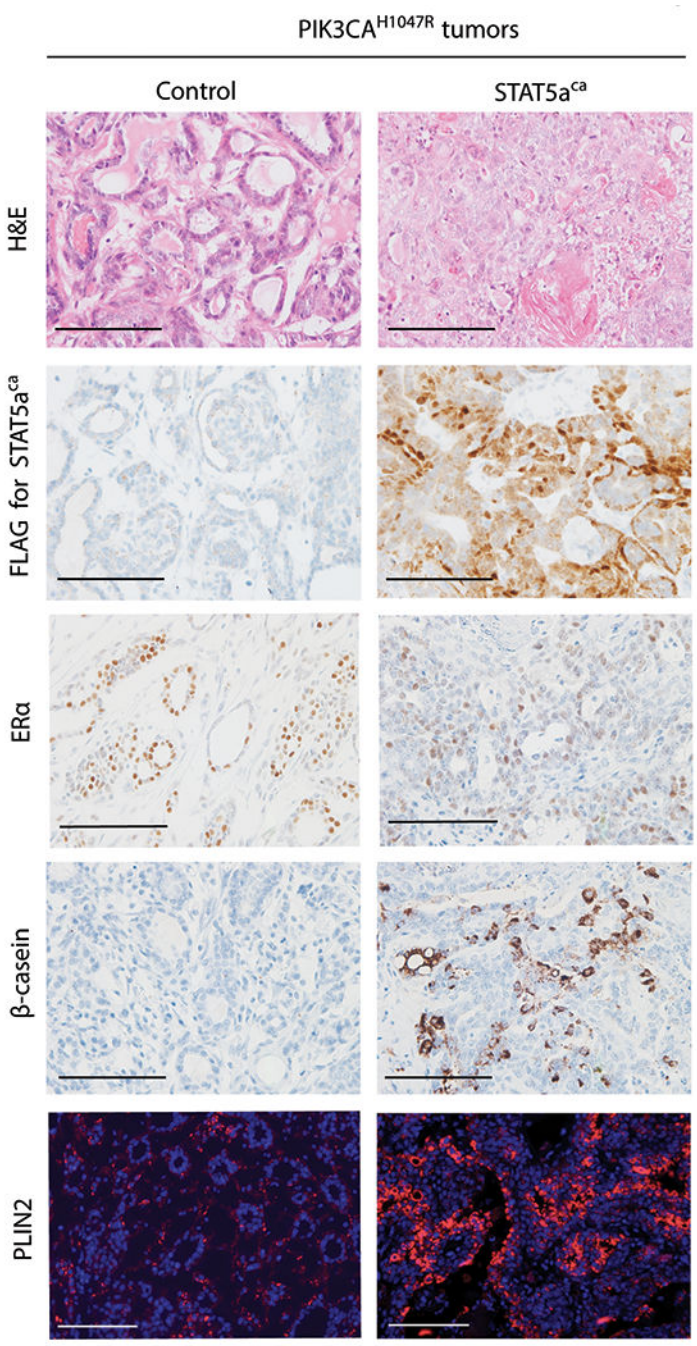

Figure 2. STAT5a^{ca} causes functional differentiation of mammary tumors initiated by *PIK3CA^{H1047R}*.

Representative images of tumor sections stained by H&E and for the indicated markers. Scale bars: 100 μm. N = 6-8.

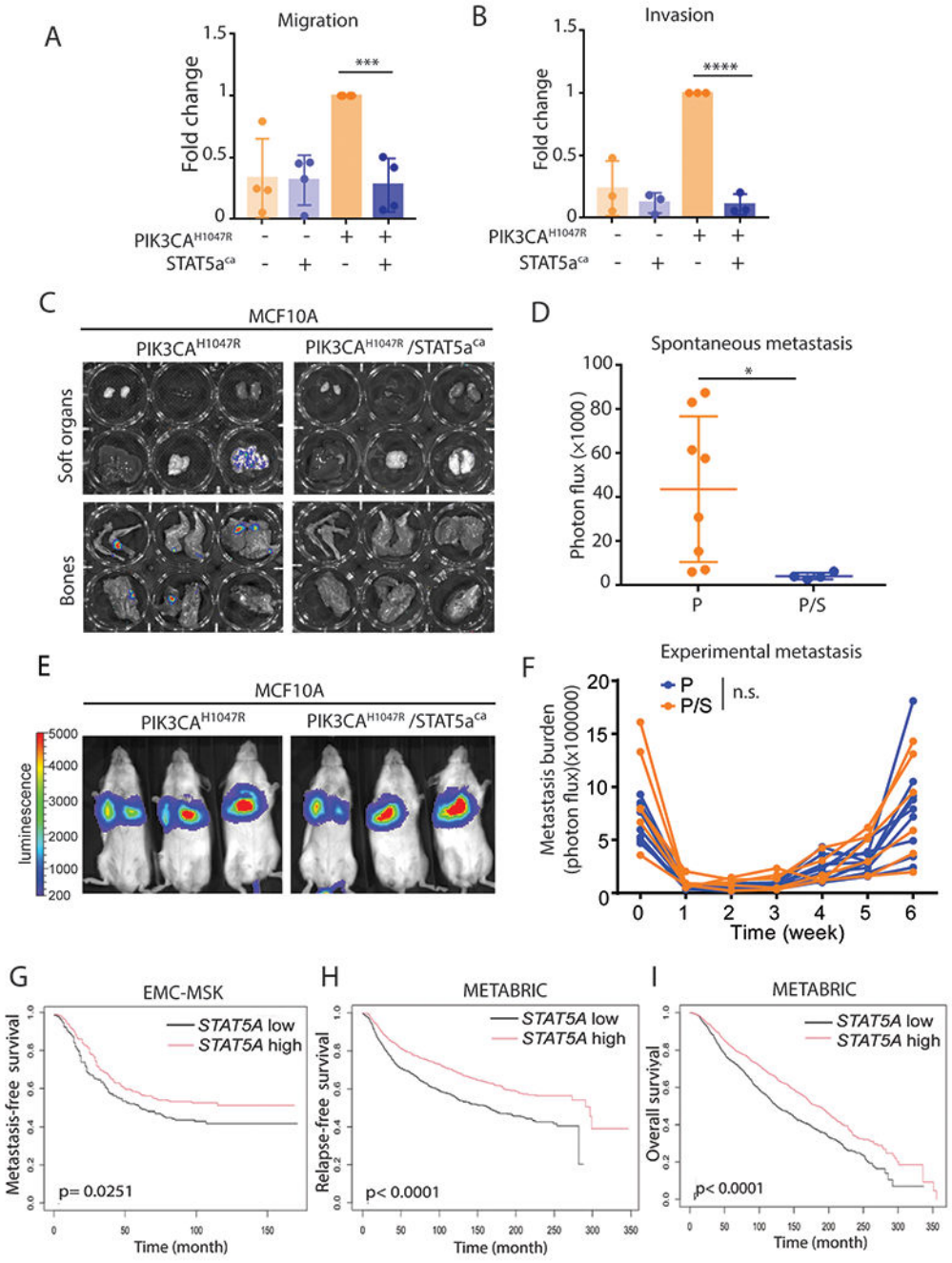

Figure 3. STAT5a^{ca} restricts the metastatic potential of human breast tumor cells, and higher *STAT5a* levels are associated with better prognosis of patients.

(A&B) Dot plots showing the migration and invasion of MCF10A cells carrying the indicated genes. Values in Y-axis are normalized to the PIK3CA^{H1047R} group. The number of biological replicates is indicated by the filled circles. The Student's *t* test was used. ***$P < 0.001$, ****$P < 0.0001$.

(C) Representative images of bioluminescence signals in the soft organs (upper panel: ovaries, spleen, kidneys; lower panel: liver, brain, lungs) and bones from mice implanted with MCF10A cells carrying PIK3CA^{H1047R} (P) or PIK3CA^{H1047R}/STAT5a^{ca} (P/S).

(D) Quantification of combined signals in (C). The Student's *t* test was used. * $P < 0.05$. Each filled circle represents a mouse. P, PIK3CA^{H1047R} (N = 8); P/S, PIK3CA^{H1047R}/STAT5a^{ca} (N = 4).

(E) Representative images of bioluminescence signals in the NSG mice at 6 weeks post tail vein injection of MCF10A cells carrying PIK3CA^{H1047R} or PIK3CA^{H1047R}/STAT5a^{ca}.

(F) Quantification of the metastasis burden. Each filled symbol represents a mouse. P, PIK3CA^{H1047R} (N = 8); P/S, PIK3CA^{H1047R}/STAT5a^{ca} (N = 6). Values in Y-axis are photon flux from lungs of individual animals.

(G) Kaplan-Meier plot of metastasis-free survival of patients stratified according to tumor *STAT5A* mRNA expression in the EMC-MSK dataset (N = 557). The patients were assigned into high or low *STAT5A* group using the median of *STAT5A* mRNA expression as the cutoff.

(H&I) Kaplan-Meier plots of relapse-free survival (G) and overall survival (H) of patients stratified according to tumor *STAT5A* mRNA expression in the METABRIC Dataset (N = 1 903). The patients were assigned into high or low *STAT5A* group using the median of *STAT5A* mRNA expression as the cutoff.

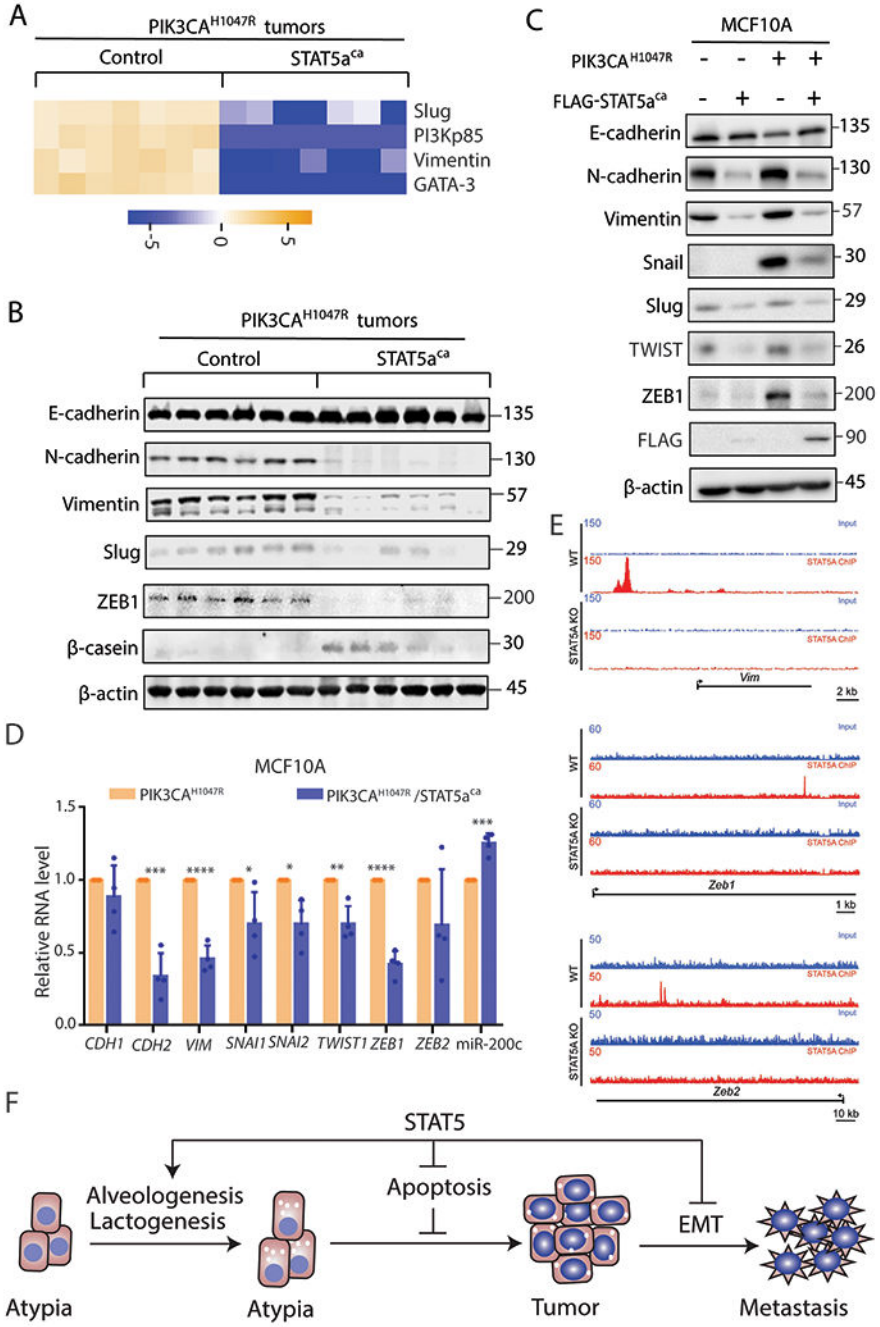

Figure 4. STAT5a^{ca} suppresses breast cancer EMT.

(A) The top 4 proteins decreased in PIK3CA^{H1047R}/STAT5a^{ca}+ tumors detected by RPPA. N = 7.

(B & C) Western blotting for the indicated proteins.

(D) Real-time PCR analysis for the indicated genes and miRNA. Data were normalized to the paired MCF10A-PIK3CA^{H1047R} group. mRNA was normalized to human acidic ribosomal protein (hARP). miR-200c was normalized to miR-103a. Student's t test was used and n = 4. * $P < 0.05$, ** $P < 0.01$, *** $P < 0.001$, **** $P < 0.0001$

(E) ChIPseq data showing STAT5 binding to both the promoter and gene body region of *Vim*, and the gene body of *Zeb1* and *Zeb2*.
(F) Model depicting the dichotomous impact of STAT5 on breast cancer formation and metastasis. While promoting tumorigenesis by lowering the apoptosis anticancer barrier, STAT5 also defines an alveolar differentiation fate (white dots), preventing EMT and metastasis.